A Novel Architecture for Multilane-Free-Flow Electronic-Toll-Collection Systems in the Millimeter-Wave Range

Wern-Yarng Shieh, Wei-Hsun Lee, Shen-Lung Tung, and Chung-Ding Ho

***Abstract*—An architecture for simultaneously performing multitarget tracking and multidata communication suitable for millimeter-wave multilane-free-flow electronic-toll-collection (ETC) systems is presented. This architecture combines the idea of frequency multiplexing in communication systems and the technique of target tracking in the pulse-Doppler radar. For target tracking, we make use of pulse ranging by the aid of pulse compression and fine target-direction determination by amplitude comparison to obtain high resolution in the radial direction (down-range), as well as both lateral directions (cross ranges). This architecture can be utilized for both active and passive onboard-unit (OBU) systems. Another important advantage of this architecture is that it can easily identify the passing vehicles not equipped with an OBU. This will activate some subsequent enforcement activities against the violation vehicles.**

***Index Terms*—Electronic toll collection (ETC), intelligent transportation system (ITS), millimeter wave, multilane free flow, short-range communication.**

I. Introduction

THERE are two major types of electronic-toll-collection (ETC) systems currently used in the world, namely single-lane and multilane free flow. It is well known that multilane-free-flow systems represent much greater complexity than single-lane systems, but the former is more convenient for faster traffic throughput, especially in high-traffic-loading areas due to less restriction on vehicle passing speed. For communication between roadside units (RSU) and onboard units (OBU) in ETC systems, there are several different media being utilized, such as 900-MHz, 2.4-GHz, and 5.8-GHz microwave based on dedicated short-range communication (DSRC), as well as 870-nm infrared.

To the authors' knowledge, a practical multilane-free-flow system employing infrared is not yet available. For microwave systems, there are several currently in use or having been tested, for example, the systems described in [1]–[4]. The method proposed by Walker and Brockelsby [1] uses in-pavement antennas and tags mounted on the lower edges of the front license plates with carrier frequency 915 MHz (or an alternate frequency 2.45 GHz). Its available communication length is 1-m long; for a vehicle with a speed of 100 km/h, it can provide only 36 ms for data communication. This is insufficient for huge-amount data transmission generally occurring in ETC applications. The system evaluated in Thessaloniki, Greece [2] employs two-stage data transmission with a carrier frequency of 5.8 GHz. The first stage is between the OBU and a first RSU for the purpose of toll collection; the second stage is another data communication between the same OBU and a second RSU to check the validity of payment, in order to identify illegal passages for enforcement. The idea of two-stage data transmission is commonly employed in microwave multilane-free-flow ETC systems, such as in [3] and [4]. The system reported in [3] uses two gantries (first and second) separated a few meters apart in tandem to mount the first and the second antenna of each traffic lane, respectively. When vehicles are traveling between these two gantries, a real-time tracking camera mounted on the center of the second gantry tracks the trajectory of each vehicle with analog optical images. The purpose of this vehicle-trajectory tracking is to discriminate vehicles which change traffic lanes when they pass through the toll-collection plaza, in order to perform the electronic payment correctly. Another two-stage data-transmission (two-gantry) system is in Singapore with a carrier frequency of 2.45 GHz [4]. In addition to the antennas (RSUs) on each traffic lane, they use additional antennas mounted interlaced between contiguous lanes to provide overlapping communication areas, in order to allow reliable communication and, at the same time, recognize the vehicle position with the antenna number. The above two systems ([3] and [4]) use different methods to obtain the trajectories or positions of passing vehicles to perform multilane-free-flow ETC.

An alternative to the abovementioned short-range communication systems known as vehicle positioning system (VPS) was recently proposed. This alternative method utilizes the Global Positioning System (GPS) and long-distance communication to perform electronic payments [5]. However, owing to the high precision requirement for vehicle positioning in ETC applications and problems associated with GPS signal outages, this technique is still not sufficiently matured for practical application. Also, the bandwidth of current microwave systems whose carrier frequencies are only up to 5.8 GHz is not sufficient

Manuscript received April 1, 2004; revised January 26, 2005. The Associate Editor for this paper was C. Nwagboso.

W.-Y. Shieh is with the Department of Electronic Engineering, St. John's University, Tamsui, Taipei County, Taiwan 25135, R.O.C. (e-mail: shiehwy@mail.sju.edu.tw).

W.-H. Lee is with the Research Institute of Chunghwa Telecom, Taoyuan, Taiwan 326, R.O.C. He is also with the Department of Computer Science, National Chiao Tung University, Hsinchu, Taiwan 300, R.O.C. (e-mail: leews@cht.com.tw).

S.-L. Tung and C.-D. Ho are with the Research Institute of Chunghwa Telecom, Taoyuan, Taiwan 326, R.O.C. (e-mail: tung168@cht.com.tw; hcdyjm@cht.com.tw).

Digital Object Identifier 10.1109/TITS.2005.853708

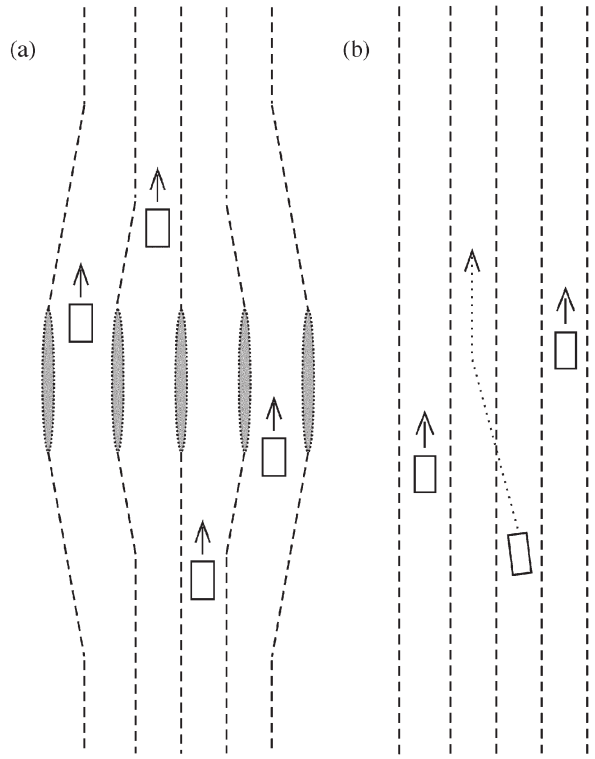

Fig. 1. ETC plaza of (a) single-lane and (b) multilane free-flow systems.

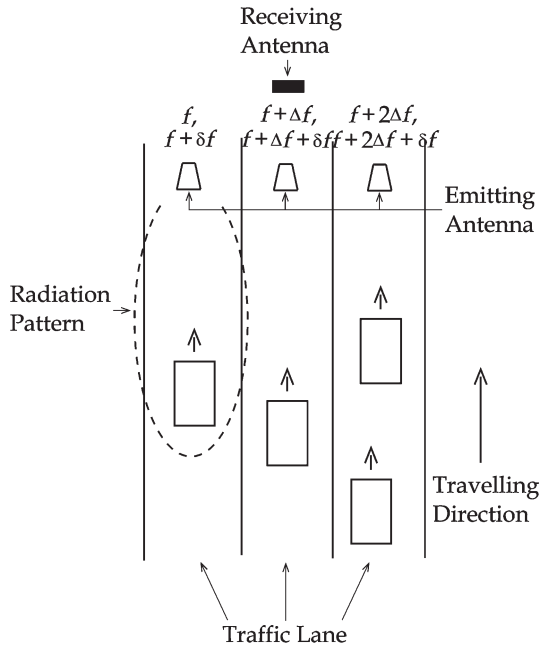

Fig. 2. Separate emitting antennas and the frequency bands used for different traffic lanes, together with a single receiving antenna for common use in millimeter-wave ETC systems.

for large-scale data communication. Obviously, it is better to provide wider bandwidth; this can be achieved more easily at higher carrier frequencies, such as those in the millimeter-wave range. In this frequency range, there have been many intelligent-transportation-system (ITS) applications. Moreover, many of them make use of some technologies originally developed in radar systems, which have been well tested in military applications for a long time [6]–[8].

In this paper, we suggest a novel architecture aimed at performing multilane-free-flow ETC by employing communication in the millimeter-wave range and methods developed in radar systems. This architecture can provide a very wide communication bandwidth and is suitable for both active and passive OBU systems.

II. The Architecture

The fact that in both multilane-free-flow and single-lane ETC systems there are huge volumes of data in several simultaneous message traffic between RSUs and OBUs in all traffic lanes is without further discussion. In multilane-free-flow systems, the vehicle passing through the data-communication region in the ETC plaza may change travel lanes during data transmission between its OBU and the RSU on the previous travel lane. Because of this, the data transmission between the OBU and the RSU on the previous travel lane may very often be incomplete and must be performed consecutively by the RSU mounted on the current travel lane, into which the vehicle has entered [see Fig. 1(b)]. This is the main difference between multilane-free-flow and single-lane systems.

Hence, the trajectories of moving vehicles passing through the data-communication region in the ETC plaza before, during, and after each data communication event are very important information for correctly performing ETC transactions in multilane-free-flow systems. This is to say that besides the simultaneous data communication between RSUs and OBUs in all traffic lanes, we also need to track all vehicles passing through the toll-collection plaza like an active seeker in an advanced missile. The purpose of vehicle-trajectory tracking is to decide the timing for separating the whole data transmission into several segments so as to be able to communicate in contiguous traffic lanes consecutively, while the vehicles change traffic lanes. The technology of multitarget tracking has been well developed in radar systems. An abundance of data-transmission techniques is also available. Now, we discuss the essence of this architecture, which combines frequency multiplexing and two techniques widely used in radar systems, including pulse ranging and fine target-direction determination.

A. Frequency Multiplexing and Wave Emission

The architecture for simultaneously performing multitarget tracking and multidata communication between vehicles and the ETC system is based on the idea of using different carrier frequencies for different purposes. Fig. 2 shows an example of frequency multiplexing [9] for an appropriate frequency-band arrangement among different traffic lanes. This figure illustrates that we use separate emitting antennas for each traffic lane, but only one common receiving antenna for collecting all return signals. The frequency bands utilized in different traffic lanes are distinguishable. There is a frequency discrepancy Δf between contiguous lanes. Furthermore, the carrier frequencies for target tracking and data transmission in each traffic lane are also different. The difference between them is δf. The radiation pattern of each emitting antenna covers approximately one traffic lane, as the dotted ellipse in the leftmost lane of

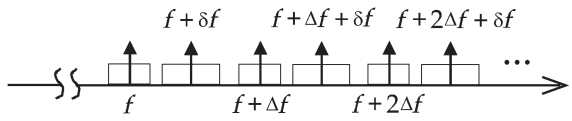

Fig. 3. Arrangement of frequency bands for simultaneously performing multitarget tracking and multidata communication in millimeter-wave ETC systems.

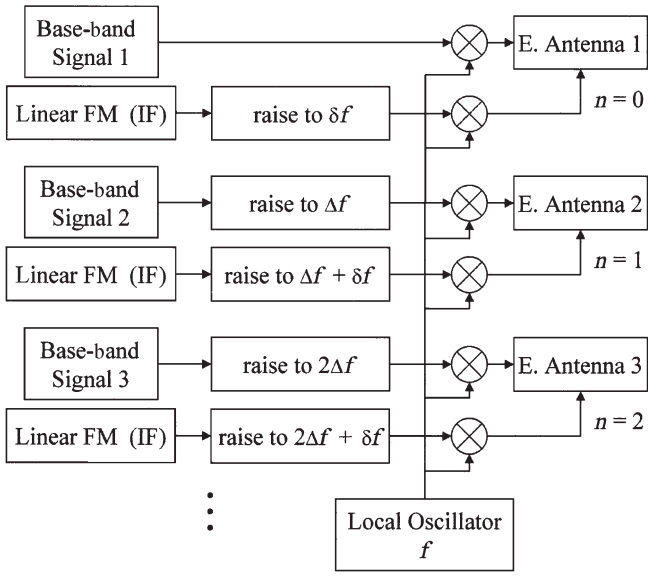

Fig. 4. Block diagram of the transmitter.

Fig. 2 shows. The arrangement of frequency bands for this architecture is shown in Fig. 3.

Fig. 4 shows a simple block diagram of the transmitter of our architecture. A local oscillator creates a continuous wave of frequency f. This frequency is allotted to lane 1 for data transmission, i.e., the baseband data-communication signal is mixed with it directly. The carrier frequency for target tracking in this lane is assigned $f + \delta f$. For target tracking, we need a linear frequency modulation (linear FM) in the intermediate-frequency (IF) band, in order to perform pulse compression in the receiver, as will be discussed later in Section II-C. We do this at frequency δf and then raise it to $f + \delta f$ by mixing it with the local oscillator. Finally, these two signals at f and $f + \delta f$ are combined and sent to the emitting antenna.

The frequency bands utilized in other traffic lanes are raised by Δf in turn. Hence, the baseband data-communication signal and the IF band tracking signal in each lane should first be raised to $n\Delta f$ and $n\Delta f + \delta f$, respectively, where $n = 0, 1, 2, 3, \ldots$ for lane 1, lane 2, lane 3, lane 4, …, in turn. These are shown in the blocks "raise to $n\Delta f$" and "raise to $n\Delta f + \delta f$" in Fig. 4. For doing all of these, we need two other local oscillators with frequencies δf and Δf, a frequency multiplier, as well as some other mixers, which are implicitly included in each block, and not shown explicitly. All these signals at frequencies $n\Delta f$ and $n\Delta f + \delta f$ are then mixed with the local oscillator f. Finally, in each traffic lane, the signals in the target-tracking channel and the data-transmission channel are combined and sent to the emitting antenna. The result is that the carrier frequencies for downlink data transmission are

$$f + n\Delta f \tag{1}$$

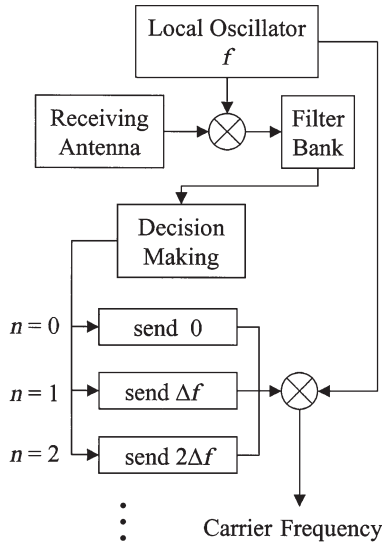

Fig. 5. Block diagram for choosing an uplink carrier frequency in an active OBU.

where $n = 0, 1, 2, 3, \ldots$ for lane 1, lane 2, lane 3, lane 4, …, in turn, and the carrier frequencies for target tracking are

$$f + n\Delta f + \delta f \tag{2}$$

also $n = 0, 1, 2, 3, \ldots$, in turn, for each traffic lane.

Here, the purpose of the target-tracking channel is to construct a high-resolution monopulse radar [10], [11]—we can obtain the target distance from pulse ranging and target direction from amplitude comparison, as will be discussed later.

B. Active and Passive OBU Systems

The OBU of the current microwave ETC systems can be divided into two categories, active and passive. During the uplink data transmission in passive systems, the emitting antenna of each roadtop unit[1] emits a continuous wave. The OBU mounted in the vehicle receives this wave, digitally modulates it, then sends it back; whereas in active systems, the OBU can actively emit uplink signals.

In our architecture, we use different frequency bands in different traffic lanes (see Fig. 2). Therefore, in passive systems, the carrier frequencies of the reflected uplink signal from different traffic lanes are automatically distinguished. For active systems, the OBU can be endowed with the ability of choosing one of several preselected frequencies as the carrier frequency for uplink data transmission, according to its previously received downlink carrier frequency. This can be realized, for example, as shown in Fig. 5. The received downlink signal from the receiving antenna after down conversion can be sent to a filter bank or a fast-Fourier-transform (FFT) analyzer to determine the received downlink carrier frequency. Then, according to this frequency, we can choose a corresponding uplink carrier frequency, this is the task of the "Decision Making" block in Fig. 5. Clearly, this function will greatly

[1]Because the RSU (the commonly accepted name) is mounted above the traffic lane, in our case (see Fig. 2), we chose to call it "roadtop unit."

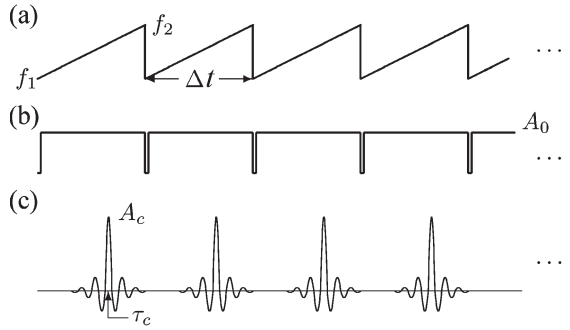

Fig. 6. Linear FM (a) repeated linear chirp-up FM from f_1 to f_2 with period Δt, (b) the received wide pulse before pulse compression with amplitude A_0, and (c) the compressed pulse received by the receiver after pulse compression with peak amplitude A_c, the time interval between the zero crossings is τ_c, which is defined as the pulsewidth.

increase the circuitry complexity compared with that of passive systems. Nevertheless, for both cases in our architecture, the uplink signals from vehicles in different traffic lanes can be distinguished without difficulty by their carrier frequencies.

C. Pulse Ranging With Pulse Compression—High Resolution in Radial Direction (Downrange)

Pulse ranging, which extracts the information of target distance from the time delay of returned signals, is a conventional method employed in radar systems. To obtain high resolution, it is necessary to use short pulsewidth. Pulse compression can compress a frequency-modulated signal to a very short pulse to achieve the requirement of high downrange resolution [10], [11]. In this paper, we will discuss the compression of linear FM signals only. Its basic concept can be found in a classical paper [12].

We send, for example, a repeated linear chirp-up frequency-modulated signal, as shown in Fig. 6(a). The time variation of frequency is from f_1 to f_2 within the period Δt, i.e., its pulse repetition frequency (PRF) $f_p = 1/\Delta t$. Clearly, the returned signal has the same composition—the portion with instantaneous frequency f_1 arrived first, followed successively by others with frequencies between f_1 and f_2. If, in the receiver, we have a device in which the components of higher frequencies (near f_2) travel faster than the lower ones (frequencies near f_1), then the returned signal can be "squeezed" into a very short pulse. Such a device is called a delay line and can be realized by several methods. One of them, which is very often encountered in radar systems, is the surface-acoustic-wave (SAW) device [10], [11].

For a linear FM pulse with constant amplitude A_0 and pulsewidth Δt [see Fig. 6(b), the time gaps between the wave repetitions are assumed to be very narrow], the compressed waveform is sinclike [12], as shown in Fig. 6(c). We define the compressed pulsewidth τ_c as the time duration between the zero crossings of the main pulse. This compressed pulsewidth τ_c is determined by the bandwidth of the FM $\Delta f \equiv f_2 - f_1$ [11], [12], i.e.

$$\tau_c = \frac{2}{\Delta f}.$$

And the ratio of the peak-power amplitudes after and before compression is [12]

$$\frac{A_c}{A_0} = \Delta t\, \Delta f$$

where the meanings of A_c and A_0 are as shown in Fig. 6. Hence, for instance, if we use a carrier frequency of 89.8 GHz and bandwidth of 400 MHz, i.e., $f_1 = 89.6$ GHz and $f_2 = 90$ GHz, then $\tau_c = 5$ ns. This leads to a downrange resolution of about 40 cm, which is sufficient for ETC application. Then, we choose a PRF $f_p = 5$ MHz, i.e., $\Delta t = 200$ ns. This leads to a range unambiguity of 60 m, which is sufficient for ETC application. With this example, the pulsewidth after compression can be reduced to $1/40$ ($\tau_c/\Delta t = 1/40$), and the received peak power can be raised 80 times, i.e., 19 dB ($A_c/A_0 = 80$). Moreover, for PRF $f_p = 5$ MHz, the range of Doppler-frequency unambiguity is also 5 MHz. Only objects with 25-Mach speed can have such high Doppler frequency for a 90-GHz incident wave; a vehicle with a speed of 270 km/h only produces a 45-kHz shift. Hence, we can say that the maximum velocity of automobiles is not restricted by this design.

With a 40-cm resolution, it is not difficult to distinguish two cars closely in tandem. On the other hand, however, with such high resolution we can also distinguish the signals reflected from different parts of a vehicle, say, from the hood and the top. Therefore, it is necessary to collect radar images of different types of vehicles by measurement in advance in this frequency range.

Finally, to obtain high resolution in the radial direction, besides the analog technique mentioned in this section, it is also possible to use digital pulse compression, such as pseudo-random codes. Its basic concepts can be found in general radar textbooks [10], [11] and will not be discussed here.

D. Fine Target-Direction Determination—High Resolution in Lateral Directions (Cross Ranges)

Having obtained a high resolution in the radial direction, we now introduce high resolution in another two lateral directions, i.e., cross ranges. This can be achieved by amplitude comparison in an antenna module with a suitable design. Although this method for fine target-direction determination has been widely used in advanced radar systems [10], [11], we describe it briefly for readers who are unfamiliar with angle tracking in such systems. We begin with an example design; this design is also suitable for ETC applications.

Fig. 7 sketches a typical layout of the slot array on the panel of a slot-array antenna, which is commonly used in an airborne Doppler radar for target-direction determination and angle tracking. In general, the panel of such an antenna is divided into four parts, quadrant 1, quadrant 2, quadrant 3, and quadrant 4 (called I, II, III, and IV, respectively, in our discussion), in order to determine the direction of the target relative to the antenna normal—elevation angle and azimuth angle.[2] For the purpose of simplifying our discussion, initially

[2]In some seekers, mainly for face-to-face (antiship) missiles, the antenna panel is divided into two parts, right and left, for determination of the azimuth angle only.

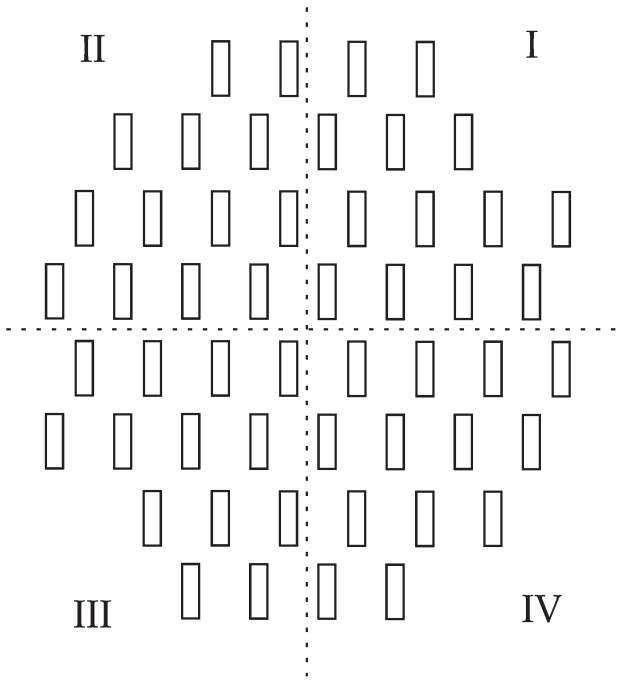

Fig. 7. Typical layout of the slot array on the panel of a slot-array antenna.

assume that the slot array on the antenna panel is divided into two parts, right and left, i.e., I + IV and II + III in Fig. 7, to determine the azimuth angle only. The strongest emitting and receiving directions of these two parts are not in the direction of the normal to the antenna, but have a tilt angle ϕ relative to it in both directions. Fig. 8(a) shows a simulated radiation (receiving) pattern calculated by a $\cos^n$ function with a tilt angle ϕ in both directions. The $\cos^n$ function is widely used in antenna-pattern simulation [13]. It has also been successfully utilized to predict the radiation pattern of the infrared-radiation module [14], [15]. In this example, we simulate the pattern of both parts of the antenna with a $\cos^3\theta$ function, which leads to a half-power beam width of 75° and a gain of 8.6 dBi. For tilt angle $\phi = 30^\circ$

$$S_R = \frac{1}{2}\cos^3\left(\theta - \frac{\pi}{6}\right)$$

$$S_L = \frac{1}{2}\cos^3\left(\theta + \frac{\pi}{6}\right)$$

wherein $(-\pi/2) < \theta < (\pi/2)$. The results are sketched by two solid loops S_{R} and S_{L}, respectively, in Fig. 8(a).

Now, define the azimuth signal-strength difference Δ_{A} as the subtraction of these two signal strengths received in some direction, i.e., $\Delta_{\mathrm{A}} = S_{\mathrm{R}} - S_{\mathrm{L}}$, and the signal-strength sum Σ as the summation of these two signal strengths, i.e., $\Sigma = S_{\mathrm{R}} + S_{\mathrm{L}}$. The results of Δ_{A} and Σ as a function of target direction angle θ are shown in Fig. 8(b) and (c), respectively. It is clear that if the target is in the direction $\theta = 0$, then $\Delta_{\mathrm{A}} = 0$ and Σ has a maximum value, therefore, $\Delta_{\mathrm{A}}/\Sigma = 0$. If the target is on the right side of the antenna normal, then $\Delta_{\mathrm{A}}/\Sigma > 0$ and the value of $\Delta_{\mathrm{A}}/\Sigma$ increases with increasing θ. When the target is on the left side of the antenna normal, then $\Delta_{\mathrm{A}}/\Sigma < 0$, and similarly, $|\Delta_{\mathrm{A}}/\Sigma|$ increases with increasing $|\theta|$. Hence, we can easily determine the azimuth angle of the

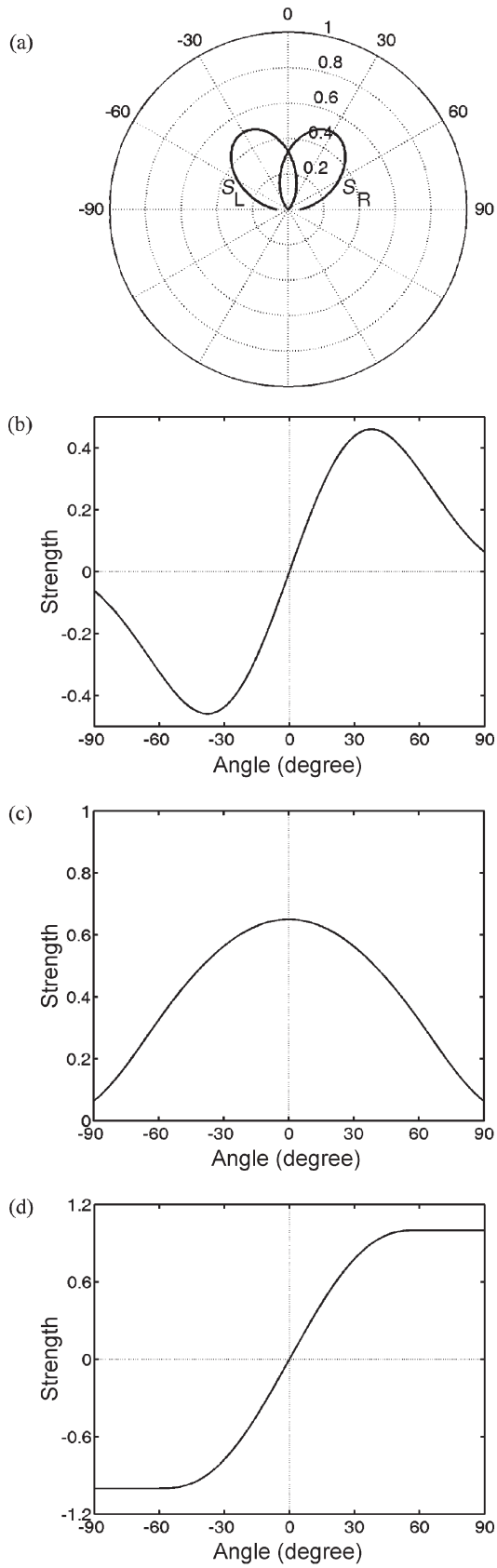

Fig. 8. (a) Typical pattern of the right and the left part of an amplitude-comparison antenna simulated by $\cos^3$ function, the tilt angle of each part is 30°, i.e., $S_{\mathrm{R}} = (1/2)\cos(\theta - (\pi/6))$, $S_{\mathrm{L}} = (1/2)\cos(\theta + (\pi/6))$, (b) the difference pattern $\Delta_{\mathrm{A}} = S_{\mathrm{R}} - S_{\mathrm{L}}$, (c) the sum pattern $\Sigma = S_{\mathrm{R}} + S_{\mathrm{L}}$, and (d) the pattern of $\Delta_{\mathrm{A}}/\Sigma$.

target from the value of Δ_A/Σ. Fig. 8(d) shows the values of Δ_A/Σ for this example. It is a monotonic function and is nearly linear for $-30^\circ < \theta < 30^\circ$. Clearly, for a target within $\pm 30^\circ$, the direction of the target can be determined without difficulty in this case. Furthermore, such an antenna module is easy to realize by using a patch antenna with a hybrid ring or slot-array antenna with a magic-T junction [16], [17].

Obviously, if we divide the antenna panel into upper and lower halves, i.e., I + II and III + IV in Fig. 7, the target elevation angle can easily be obtained by the same method. By combining the azimuth angle and the elevation angle, the direction of the target relative to the antenna can be determined. Referring to Fig. 7, if the received signal strengths of the four quadrants are S_I, S_{II}, S_{III}, and S_{IV}, respectively, then by defining

$$\Delta_A \equiv (S_I + S_{IV}) - (S_{II} + S_{III})$$
$$\Delta_E \equiv (S_I + S_{II}) - (S_{III} + S_{IV})$$
$$\Sigma \equiv S_I + S_{II} + S_{III} + S_{IV}$$

the value of Δ_A/Σ gives the azimuth angle of the target, and the value of Δ_E/Σ gives the elevation angle. Combining these two data, the direction of the target can be obtained.

There is one important thing worth pointing out; because vehicles travel on two-dimensional roads, their degrees of freedom are two. Under this condition, the precisely detected target direction by amplitude comparison can also be used to determine the target position relative to the receiving antenna, by the aid of a simple geometric relation. This result can be combined with the result of the pulse ranging mentioned above to enhance the validity. Furthermore, we can easily estimate the target velocity from the consecutive information of the target position. Therefore, the Doppler-frequency-shift discrimination for obtaining target velocity is unnecessary. This can greatly simplify the implementation of our architecture.

E. Frequency-Band Arrangement

From the analysis in Section II-C, we understand that for a range resolution of 40 cm, we need a 400-MHz bandwidth in each target-tracking channel. If we provide 90 MHz for data transmission in each data-communication channel (currently, in 5.8-GHz DSRC systems, the bandwidth for data transmission is only 10 MHz) and another two 5 MHz for guard bands to prevent interference, then each traffic lane needs 500-MHz bandwidth. That is, in (1) and (2), $\Delta f = 500$ MHz and $\delta f = 250$ MHz. For a four-lane highway we need a total of 2-GHz bandwidth, say, from 89.0 to 91.0 GHz, as shown in Fig. 9. In this figure, we illustrate a sample design of frequency-band arrangement; the 90-MHz bands are for data transmission, and the 400-MHz bands for target tracking. Between contiguous bands, there is a 5-MHz guard band.

III. Receiver—The Procedure of Signal Processing

The signal-processing procedure can be easily understood by referring to Fig. 10, which shows the block diagram of the receiver of our architecture. The arrangement of the frequency bands for different traffic lanes was discussed in Sections II-A and II-E. Now, we concentrate on the receiver of our architecture. Because the procedures for determining the azimuth and the elevation angle are the same, it is enough to illustrate just one of them. Following the above context, we discuss the azimuth part further. The procedure for obtaining the elevation angle is pursued in the same manner.

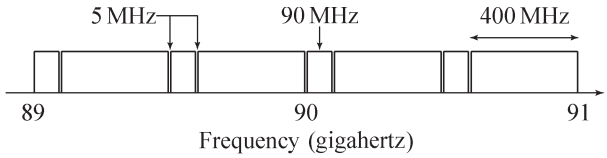

Fig. 9. Example of frequency-band arrangement for simultaneously performing multidata transmission and multitarget tracking.

A. Difference and Sum Signals

As specified previously, the return signals from all traffic lanes, including data transmission and target tracking, are collected by a single common receiving antenna. The first task of our receiver is to create the difference and the sum signal of the target, in order to obtain the target-angle information. This is performed by the "D & S Processor" block in Fig. 10, which can be realized easily by a hybrid ring for patch antennas or by a magic-T junction for slot-array antennas [16], [17]. Readers who are unfamiliar with these concepts are encouraged to refer to the quoted references.

B. Down Conversion and Baseband Signal Recovery

Owing to the division of frequency bands for different traffic lanes, as well as for target tracking and data transmission (see Figs. 2 and 3), it is necessary to single out and separate all of the abovementioned frequency intervals from one another. As shown in Fig. 10, the difference (Δ) and the sum (Σ) signals are down converted by mixing them with a continuous wave of frequency f coming from the local oscillator through a mixer. After this, we obtain all data-communication and all target-tracking signals from all traffic lanes at frequencies

$$n\Delta f + f_d$$

and

$$n\Delta f + \delta f + f_d$$

where f_d is the Doppler frequency shift, which is dependent on the velocity of the vehicles due to their motion. Then by the aid of a filter bank, which is composed of a set of bandpass filters, all signals mentioned above can be separated very easily. This filtering procedure is displayed in Fig. 10 by two "Filter Bank" blocks.

C. Final Signal Processing

Now, these separated signals at different frequency bands are at our disposal. The data-transmission signals at frequencies $n\Delta f + f_d$ are input to the data-transmission channel for decoding. In this channel, we will obtain all the uplink data sent by

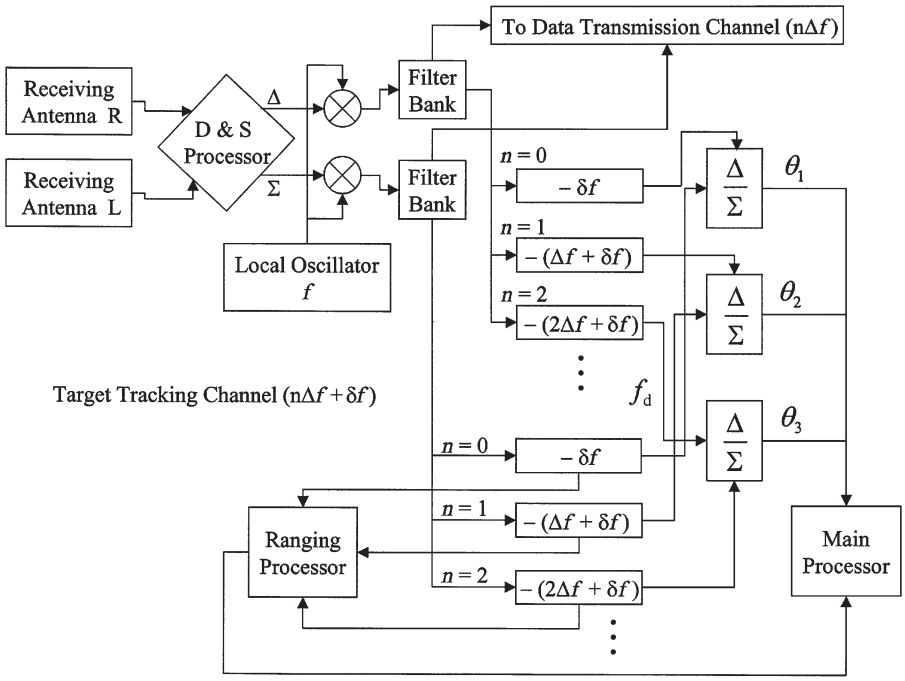

Fig. 10. Block diagram of the receiver for target tracking.

each OBU on each vehicle passing through the toll-collection plaza from different traffic lanes. Because our purpose here is to present an architecture for simultaneously performing multitarget tracking and multidata communication, the details of this channel will not be discussed further.

For target-tracking signals at frequencies $n\Delta f + \delta f + f_{\mathrm{d}}$, we have to first convert them to their original IF frequency. This is performed by the blocks "$-(n\Delta f + \delta f)$" in Fig. 10, where $n = 0, 1, 2, 3, \ldots$. After this, we perform the pulse compression procedure mentioned in Section II-C for the Σ-part of the signal, because it is stronger than the Δ part. Then, we can determine the distance of the vehicle relative to the receiving antenna from the time delay of the target echo (pulse ranging). These two steps are realized in the "Ranging Processor" block in Fig. 10. Now, we perform the division Δ/Σ separately for each traffic lane to obtain the target-angle information as shown by the "Δ/Σ" blocks.

At this stage, we have successfully obtained the information of the direction and the distance, as well as located the traffic lanes, of all vehicles traveling through the toll-collection plaza. From the time variation of these parameters, it is an easy task to sketch their trajectories and estimate their velocities. Obviously, the data communication between the ETC system and all OBUs in different traffic lanes can be performed simultaneously. Hence, with the architecture presented in this paper multilane-free-flow ETC can be completely and successfully accomplished.

Furthermore, the above discussion implicitly indicates a structure of direct conversion. However, this is not unique. In fact, it is certainly possible, and even more realistic, for such high carrier frequencies, to design with multiple-conversion superheterodyne. This paper only shows the basic concept of our architecture and omits the detail.

IV. Conclusion

The architecture presented in this paper is suitable for multilane-free-flow electronic-toll-collection (ETC) systems. The principal idea is that from the information of the trajectories of the vehicles passing through the ETC plaza, it is easy to decide the timing for separating the whole data transmission into segments so as to communicate in contiguous traffic lanes consecutively, while the vehicles change lanes. Another advantage of this architecture is that the millimeter-wave range can provide a very wide communication bandwidth to overcome the shortcoming of bandwidth deficiency present in the centimeter-wave range.

To realize this architecture, we allot different frequency bands to different traffic lanes, as well as to the different purposes of target tracking and data communication. This architecture can be utilized for both active and passive on-board-unit (OBU) systems, although for active systems, the circuitry of the OBU is more complicated. With the aid of amplitude comparison and linear frequency modulation pulse compression, the target direction can be precisely determined and the resolution in the radial direction can be 40 cm. This needs a 400-MHz bandwidth for target tracking in each traffic lane. In addition to this, if we provide 90 MHz for data transmission and two 5-MHz guard bands, then the bandwidth required by each traffic lane is 500 MHz. For a four-lane highway, we need a total of 2-GHz bandwidth, say, from 89 to 91 GHz. With a 40-cm resolution, it is not difficult to distinguish two cars closely in tandem. However, with such high resolution, we can also distinguish the signals reflected from different parts of a vehicle. Therefore, it is necessary to collect radar images of different types of vehicles by measurement in advance in this frequency range.

Owing to the two-dimensional movement of traveling vehicles, the target direction obtained by amplitude comparison is sufficient to determine the target distance relative to the receiving antenna by the aid of a simple geometric relation. This can be combined with the result of pulse ranging to enhance the reliability. Another very important advantage of this architecture is that it can easily identify passing vehicles not equipped with an OBU, since for such vehicles, there will be target-tracking signals in the receiver, but their uplink data-transmission signals will be absent. This information can be used to activate some subsequent enforcement activities against the violation vehicles.

ACKNOWLEDGMENT

The authors wish to express their appreciation to all their colleagues who are engaging or have engaged in the Project of Intelligent Transportation Systems at the Research Institute of Chunghwa Telecom (formerly the Chunghwa Telecommunication Laboratories). This paper is an offspring of their contribution.

REFERENCES

[1] C. M. Walker and W. K. Brockelsby, "Automatic Vehicle Identification (AVI) technology design considerations for highway applications," in *Proc. 41st IEEE Vehicular Technology Conf., Gateway to the Future Technology in Motion*, St. Louis, MO, May 19–22, 1991, pp. 805–811.

[2] M. A. S. Mustafa, M. Pitsiava-Latinopoulou, and G. A. Giannopoulos, "The multilane electronic toll collection system in Thessaloniki: Evaluation of its first 6 months of operation," in *Proc. IEEE Vehicle Navigation and Information Systems Conf.*, Yokohama, Japan, Aug. 31–Sep. 2, 1994, pp. 699–703.

[3] D.-W. Lim and J.-S. Jun, "Free-flow multi-lane ETC system using real-time individual vehicle tracking," in *Proc. 5th Asia-Pacific Intelligent Transportation System (ITS) Forum*, Seoul, Korea, Jul. 2–5, 2002, pp. TS1–TS3.

[4] H. Hashimoto, H. Ohno, M. Konishi, K. Morishita, and K. Sugimoto, "Multi-lane electronic road pricing system in Singapore," *Mitsubishi Juko Giho*, Mitsubishi Heavy Industries Ltd., vol. 36, no. 1, pp. 36–45, 1999.

[5] W.-H. Lee, B.-S. Jeng, S.-S. Tseng, and C.-H. Wang, "Electronic toll collection based on vehicle-positioning system techniques," in *Proc. IEEE Int. Conf. Networking, Sensing, and Control*, Taipei, Taiwan, R.O.C., Mar. 21–23, 2004, pp. 643–648.

[6] D. M. Grimes and T. O. Jones, "Automotive radar: A brief review," *Proc. IEEE*, vol. 62, no. 6, pp. 804–822, Jun. 1974.

[7] M. E. Russell, A. Crain, A. Curran, R. A. Campbell, C. A. Drubin, and W. F. Miccioli, "Millimeter-wave radar sensor for automotive intelligent cruise control (ICC)," *IEEE Trans. Microw. Theory Tech.*, vol. 45, no. 12, pp. 2444–2453, Dec. 1997.

[8] M. E. Russell, C. A. Drubin, A. S. Marinilli, W. G. Woodington, and M. J. Del Checcolo, "Integrated automotive sensors," *IEEE Trans. Microw. Theory Tech.*, vol. 50, no. 3, pp. 674–677, Mar. 2002.

[9] H. Taub and D. L. Schilling, *Principles of Communication Systems*, 2nd ed. New York: McGraw-Hill, 1987, ch. 3.

[10] B. Edde, *Radar—Principles, Technology, Applications*. Englewood Cliffs, NJ: Prentice-Hall, 1993.

[11] M. I. Skolnik, *Introduction to Radar Systems*, 2nd ed. New York: McGraw-Hill, 1980.

[12] C. E. Cook, "Pulse compression—Key to more efficient radar transmission," *Proc. IRE*, vol. 48, no. 3, pp. 310–316, Mar. 1960.

[13] J. D. Kraus, *Antennas*, 2nd ed. New York: McGraw-Hill, 1988, ch. 3.

[14] W.-Y. Shieh, "The analysis of single-lane OBU and RTU optmum setup configuration in automatic electronic-toll-collection systems," Inner Report of Research Institute of Chunghwa Telecom, Taipei, Taiwan, R.O.C., 89-EC-023, Nov. 2000.

[15] ——, "The comparison of the efficacy of two-piece and single-piece RTU LED-module on the down-link data transmission in our ETC system," Inner Report of Research Institute of Chunghwa Telecom, Taipei, Taiwan, R.O.C., 90-EC-001, Jan. 2001.

[16] R. S. Elliott, *An Introduction to Guided Waves and Microwave Circuits*. Englewood Cliffs, NJ: Prentice-Hall, 1993, ch. 10.

[17] R. E. Collin, *Foundations for Microwave Engineering*, 2nd ed. New York: McGraw-Hill, 1992, ch. 6.

Wern-Yarng Shieh was born in Taipei, Taiwan, R.O.C., in 1958. He received the B.Sc. and M.Sc. degrees in physics from the Chung-Cheng Institute of Technology, Taoyuan, Taiwan, in 1981 and 1985, respectively, and the Dr. Ing. degree in electrical engineering from the Technishe Universität Hamburg-Harburg, Hamburg, Germany, in 2000.

He was an Assistant Researcher, during 1985 and 1995, at the Chung-Shan Institute of Science and Technology, Taoyuan, Taiwan, R.O.C. There, he worked on radar-cross-section reduction (stealth), frequency selective surface (FSS), multilayer microwave absorber, radar-cross section far-field measurement, and radar system (seeker). From 2000 to 2005, he was a Project Researcher at the Research Institute of Chunghwa Telecom, Taoyuan, Taiwan. Now, since 2005, he is an Assistant Professor at the Department of Electronic Engineering, St. John's University, Tamsui, Taipei County, Taiwan. His current research interests are millimeter-wave short-range communication systems, antenna near-field measurement, infrared short-range communication system, intelligent transportation systems (ITS), and electronic-toll-collection (ETC) system.

Wei-Hsun Lee was born in Chiayi, Taiwan, R.O.C., in 1969. He received the B.Sc. degree in information engineering and computer science from the Feng Chia University, Taichung, Taiwan, in 1991, and the M.Sc. degree in computer science and information engineering from the National Cheng Kung University, Tainan, Taiwan, in 1993. Currently, he is working towards the Ph.D. degree in the Department of Computer Science, National Chiao Tung University, Hsinchu, Taiwan.

He has been an Associate Researcher, since 1993, at the Research Institute of Chunghwa Telecom in Taoyuan, Taiwan. His current research interests are vehicle-positioning system (VPS), data-mining technology, advanced traffic-management system, and ETC system.

Shen-Lung Tung was born in Tainan, Taiwan, R.O.C., in 1966. He received the B.Sc. degree in electronic engineering from the Chung Yuan Christian University, Taoyuan, Taiwan, in 1988 and the M.Sc. degree in electrical engineering from the National Central University, Taoyuan, Taiwan, in 1990.

He was an Assistant Researcher at the Chung-Shan Institute of Science and Technology in Taoyuan, Taiwan, R.O.C., from 1990 to 1997. There, he worked on electronic-countermeasure (ECM) research. During 1997 and 1998, he was a Senior Engineer at the Arima Computer Corporation, Taipei, Taiwan, for developing advanced notebook computers. Since 1998, he has worked at the Research Institute of Chunghwa Telecom, Taoyuan, Taiwan. His current research interests are concerned with ITS, such as millimeter-wave short-range communication system, antenna near-field measurement, dedicated short-range infrared communication system, and the ETC system.

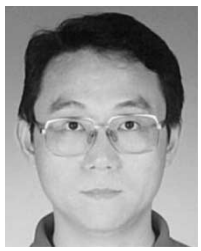

Chung-Ding Ho was born in Taipei, Taiwan, R.O.C., in 1964. He received the B.Sc. and M.Sc. degrees in communication engineering from the National Chiao Tung University, Hsinchu, Taiwan, in 1987 and 1989.

He has worked at the Research Institute of Chunghwa Telecom, Taoyuan, Taiwan, since 1989. Now, his research focuses on developing applications for ITS.